

## An Accuracy Assessment of Magellan Very Long Baseline Interferometry

D. B. Engelhardt\*, G. R. Kronschnabl\*, and J. S. Border†

Jet Propulsion Laboratory  
California Institute of Technology  
Pasadena, CaliforniaAbstract

Very Long Baseline Interferometry (VLBI) measurements of the Magellan spacecraft's angular position and velocity were made during July through September, 1989, during the spacecraft's heliocentric flight to Venus. The purpose of this data acquisition and reduction was to verify this data type for operational use before Magellan is inserted into Venus orbit, in August, 1990. The accuracy of these measurements are shown to be within 20 nanoradians in angular position, and within 5 picoradians/sec in angular velocity. The media effects and their calibrations are quantified; the wet fluctuating troposphere is the dominant source of measurement error for angular velocity. The charged particle effect is completely calibrated with S and X-Band dual-frequency calibrations. Increasing the accuracy of the Earth platform model parameters, by using VLBI-derived tracking station locations consistent with the planetary ephemeris frame, and by including high frequency Earth tidal terms in the Earth rotation model, add a few nanoradians improvement to the angular position measurements. Angular velocity measurements were insensitive to these Earth platform modelling improvements.

Introduction

The Magellan spacecraft, launched May 4, 1989, is currently on a heliocentric trajectory to Venus, with a scheduled arrival on August 10, 1990. Upon arrival, Magellan will be inserted into a nearly polar orbit in order to systematically map the surface of Venus using a Synthetic Aperture Radar (SAR). The spacecraft orbit will be determined from radiometric measurements of the spacecraft velocity; highly accurate orbit reconstruction and prediction are required to effectively command the SAR, to provide picture-element registration in the ground processing of the radar image data, and to interpret measurements from an on-board altimeter. The nominal orbit about Venus will have a relatively short orbital period (3.15 hours) and low periapsis altitude (250 km), with an eccentricity of 0.38. This orbit geometry poses a substantial challenge to navigators in determining the spacecraft orbit within the stringent accuracy requirements because (1) conventional, two-way, coherent Doppler measurements are less sensitive to certain orbit parameters, namely, the orientation of the orbit about the Earth-spacecraft line-of-sight [Wood, 1986], and (2) uncertain irregularities in the Venus gravity field will perturb the spacecraft over a large fraction of each orbit.

---

\* Member of Magellan Navigation Team, Navigation Systems Section.

† Member of Tracking Systems and Applications Section.

To meet orbit determination accuracy requirements, measurements of the spacecraft velocity in the plane-of-the-sky will be made [Mohan, 1985]. These data will provide information on the orbit parameters poorly determined with Doppler measurements, as Doppler measures the spacecraft velocity in only the spacecraft line-of-sight direction. Very Long Baseline Interferometry (VLBI) is used to provide this measurement by correlating the spacecraft radio downlink received at two widely separated ground antennas [Melbourne, 1977].

This VLBI technique has been experimentally proven with Voyager, a deep space probe [Border et al., 1982], and with Pioneer 12, a Venus orbiter [Esposito et al., 1983], but never proven operationally. To verify that the VLBI system can meet stringent operational and accuracy requirements for a planetary orbiter, a 9 week test was conducted during the early heliocentric cruise portion of Magellan's trajectory to Venus. Spacecraft and quasar VLBI measurements were acquired and processed during this time period, in a manner similar to the planned VLBI data acquisition and reduction in the orbit phase. This paper describes this test and the assessment of the VLBI measurement precision about a reference trajectory. The accuracies of the reference trajectory, the media calibrations, and the Earth platform models are presented. Their contribution to the measurement accuracy is included in the presentation of the VLBI measurement accuracy.

### Magellan Radiometric Measurements

Three types of radiometric measurements of the spacecraft state are made: 2-way coherent Doppler, Differential One-Way Range (DOR), and Differential One-way Doppler (DOD). Doppler is collected at a single station, and the DOR and DOD are VLBI measurements, made by simultaneously recording 10 minute scans of the spacecraft downlink signal at two widely separated tracking stations. NASA's Deep Space Network (DSN) tracking stations acquire and relay the data to the Jet Propulsion Laboratory in Pasadena, California. The DSN tracking stations are spaced around the globe in California, Spain, and Australia. The VLBI intercontinental baselines are between the Spain-California and California-Australia tracking stations. Figure 1 shows the DSN sites. Simplified Earth-spacecraft geometry is shown in Figure 2. This geometry is simplified by assuming a distant spacecraft, where the range,  $\rho$ , is much greater than the baseline length,  $B$ . These three data types are briefly described below.

### **Doppler**

Two-way coherent Doppler measures the spacecraft's velocity component in the line-of-sight from the antenna to the spacecraft, as shown by  $\dot{\rho}_1$  and  $\dot{\rho}_2$ , at tracking stations 1 and 2, in Figure 2. The tracking station generates and transmits a signal with a stable frequency, and the spacecraft sends a coherent version of the received signal back to the same station where the Doppler frequency shift is determined. This Doppler frequency shift is proportional to the spacecraft velocity component in the line-of-sight direction by the factor  $(c/2f)$ , where  $f$  is the signal frequency and  $c$  is the speed of light. The line-of-sight direction is specified by  $\hat{e}_1$  in Figure 2.

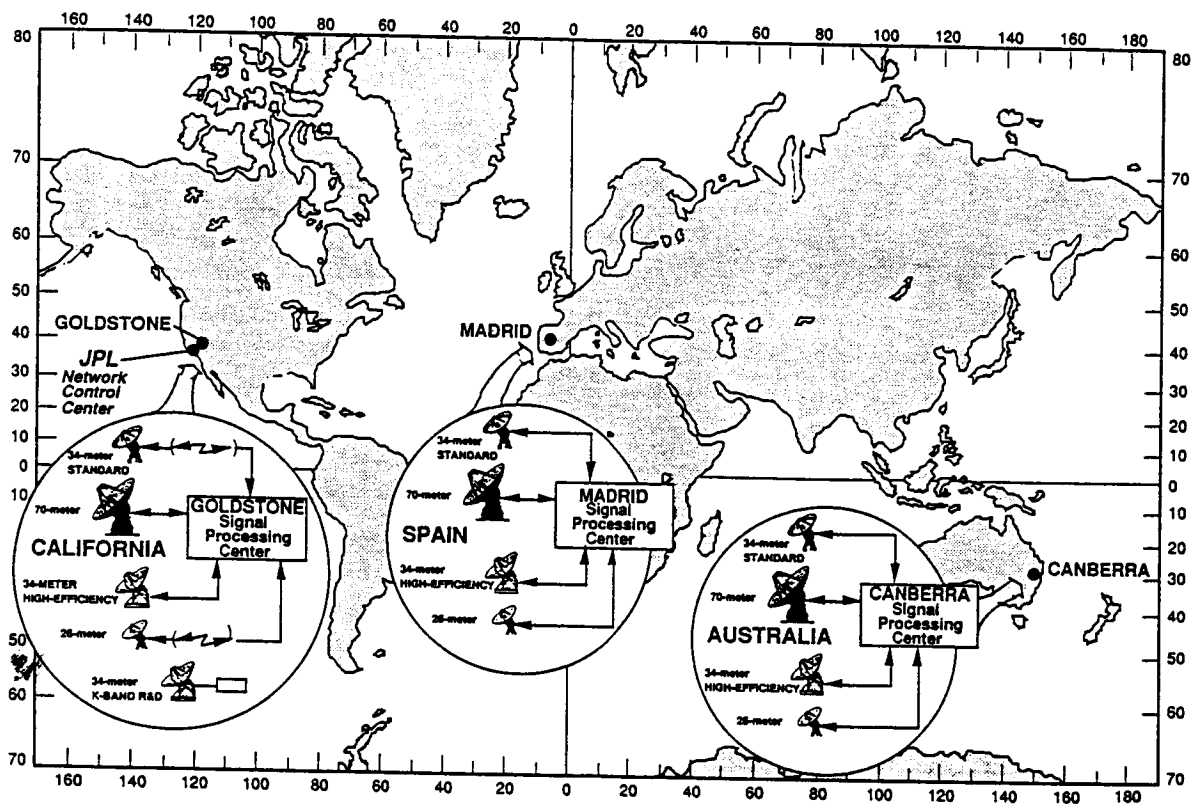


Figure 1. Deep Space Network Sites

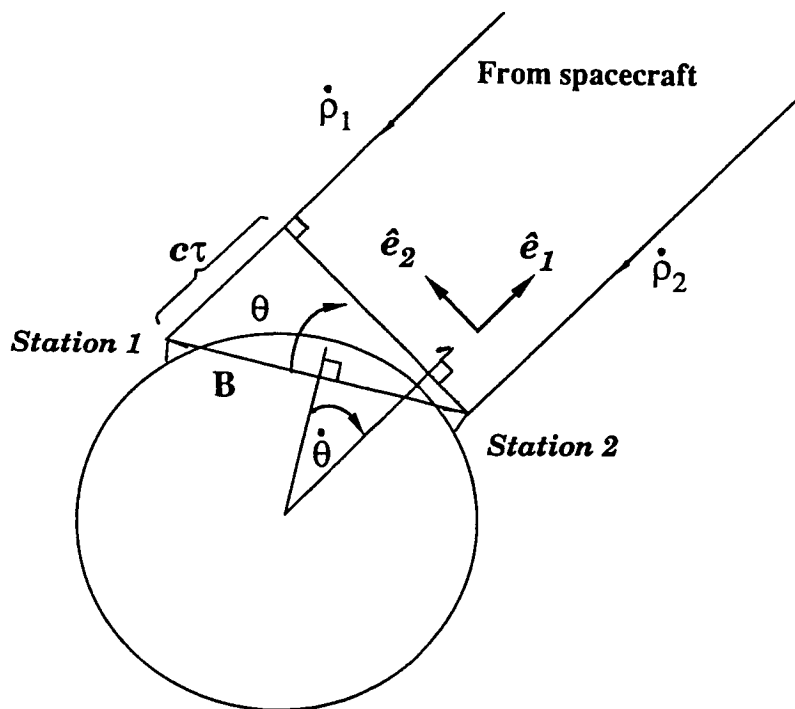


Figure 2. Simplified VLBI Geometry

## DOR

Differential One-way Range (DOR) measures the geocentric angular position of the spacecraft with respect to the baseline; this quantity is shown by  $\theta$  in Figure 2. This angle is determined by directly measuring  $\tau$ , the delay of the spacecraft signal reception from station 1 to station 2. In Figure 2,

$$c\tau \cong B \sin \theta. \quad (1)$$

Given  $B$ , the baseline length,  $\theta$  is determined from the measurement of  $c\tau$ , the differential range between stations.  $\tau$  is determined by differencing the phase of the signal received at each station [Border, 1972]. This delay is ambiguous by an integer number of cycles, however. Multiple downlink frequency tones are needed to provide the information to resolve this ambiguity. Harmonics of Magellan's telemetry subcarrier signal provide recordable side tones 2 to 35 MHz apart. The ambiguity in the 2 MHz bandwidth is  $c/2 \text{ Mhz}/B$ , or 17 microradians, and is easily resolved from apriori knowledge. The 35 MHz bandwidth provides more measurement precision.

## DOD

Differential One-way Doppler (DOD) measures the geocentric angular velocity of the spacecraft with respect to the baseline; this quantity is shown by  $\dot{\theta}$  in Figure 2. This angular rate is determined by directly measuring  $\dot{\tau}$ , the time delay-rate of the spacecraft carrier signal from station 1 to station 2. Differentiating equation (1) with respect to time gives

$$c\dot{\tau} \cong B \cos \theta (\dot{\theta}). \quad (2)$$

$c\dot{\tau}$  is the differential velocity between stations, and the sought-after rate is:

$$\dot{\theta} \cong \frac{c\dot{\tau}}{B \cos \theta} \quad (3)$$

$\dot{\theta}$  is related to the spacecraft velocity,  $\vec{V}_{s/c}$ , by:

$$\dot{\theta} \cong \frac{(\vec{V}_{s/c} \cdot \hat{e}_2)}{R} + \text{Earth rotation of baseline} \quad (4)$$

where  $R$  is the Earth to spacecraft range, and  $\hat{e}_2$  is the direction normal to the antenna-spacecraft line-of-sight, as shown in Figure 2. Assuming the earth rotation of the baseline is known, the measurement of  $c\dot{\tau}$  is related to the spacecraft velocity,  $\vec{V}_{s/c}$ , by:

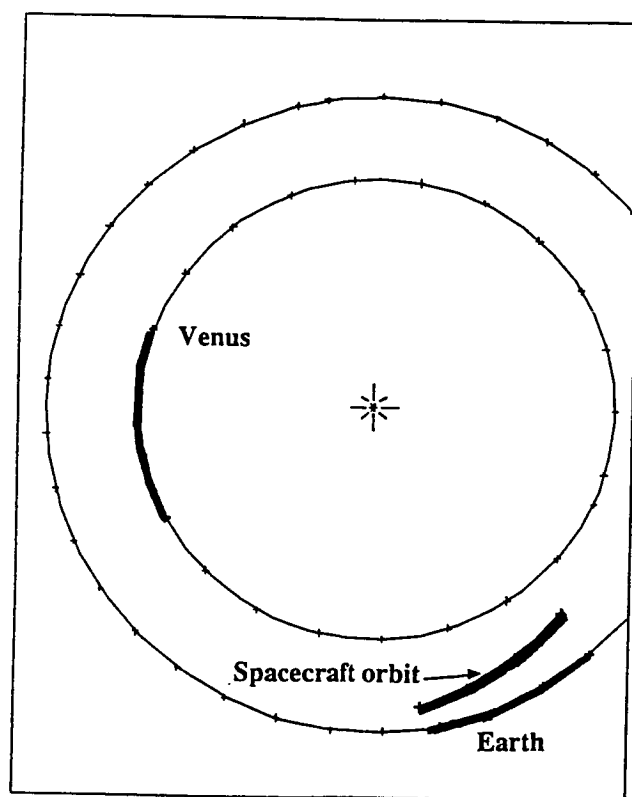
$$c\dot{\tau} \cong \frac{B \cos \theta}{R} (\vec{V}_{s/c} \cdot \hat{e}_2). \quad (5)$$

$\dot{\tau}$  is determined by rate of change of the carrier signal phase from each station.

DOR and DOD measurements can also be generated from the radio emissions of quasars for measurement calibration purposes. Quasar delay is obtained by signal cross-correlation [Thomas, 1972]. Since these quasar measurements are corrupted in almost the same way as spacecraft measurements are by tracking station location errors, media errors, and timekeeping errors, spacecraft and quasar measurements made in close temporal and spatial proximity are differenced to greatly reduce these major errors. These spacecraft-quasar differenced measurements are signified by  $\Delta$ DOR and  $\Delta$ DOD, or  $\Delta$ VLBI in general.

### The Magellan Trajectory

The radiometric data used for this accuracy analysis was collected from July 1, 1989 to August 11, 1989, early in Magellan's 15 month heliocentric cruise to Venus. The view of the spacecraft trajectory during this period, from the north ecliptic pole, is shown in Figure 3.



July 4, 1989 to August 3, 1989

Figure 3. Trajectory View from North Ecliptic Pole

The VLBI measurement accuracy is quantified as an RMS value of measurement 'residuals'. A measurement residual is the difference of the acquired measurement and a

predicted measurement. The predicted measurement is computed using a reference spacecraft trajectory and models of the Earth platform, radio frequencies, and quasar locations. So the measurement RMS quantifies the data precision about a reference trajectory. This reference trajectory accuracy has been computed, so that the absolute measurement accuracy can be ascertained. A reference trajectory was determined from Doppler and  $\Delta$ DOR data. From Equation (3), one can see that  $\theta$  is an intermediate quantity in the computation of  $\dot{\theta}$ , given the measurement of  $c\dot{r}$ . To evaluate the  $\Delta$ DOD data accuracy, then, the reference trajectory computation included  $\Delta$ DOR data, to provide direct information of  $\theta$ .

The trajectory accuracy is given in terms of uncertainty in geocentric spherical coordinates of the spacecraft on August 11, 1989 (at the end of the data arc). The right ascension,  $\alpha$ , is measured with respect to the vernal equinox of 2000.0, and the declination,  $\delta$ , is measured with respect to Earth's mean equator. These uncertainties take into account the measurement errors, as well as the known uncertainties in the station locations, spacecraft non-gravitational forces (i.e. solar radiation pressure), and quasar locations.\* The trajectory uncertainties are given in Table 1 for orbit solutions using 3 different data sets: Doppler only, Doppler+ $\Delta$ DOR, and Doppler+ $\Delta$ DOD.

	Doppler Only	Doppler + $\Delta$ DOR	Doppler + $\Delta$ DOD
Range, (km)	77.1	73.9	73.1
$\alpha$ , (nanorads)	474.1	338.4	542.5
$\delta$ , (nanorads)	724.4	303.2	558.0
Range-rate, (mm/s)	0.196	0.148	0.277
$\dot{\alpha}$ , (picorads/sec)	0.1448	0.1500	0.1410
$\dot{\delta}$ , (picorads/sec)	0.5057	0.4833	0.2926

**Table 1.** Trajectory Uncertainty on August 11, 1989, computed with three data sets: Doppler only, Doppler+ $\Delta$ DOR, and Doppler+ $\Delta$ DOD.

The strength of each VLBI data type is apparent. The  $\Delta$ DOR data brings in angular position information, reducing the angular position uncertainty by a factor of 2. The  $\Delta$ DOR data arc was only 2 weeks long, compared to a 6 week arc of  $\Delta$ DOD. For comparable data arcs, the  $\Delta$ DOR would be expected to produce by far the most accurate measure of angular velocity during cruise. The  $\Delta$ DOD data brings in angular velocity information, reducing the angular velocity uncertainty by a factor of 1.5.

\* These uncertainties are: 20% in non-gravitational force values (solar radiation pressure and unbalanced spacecraft maneuvers); 20 nanoradian radio/planetary frame-tie offset; station location errors of: 1.5 meters in distance from the pole, 1.0 meter in longitude, 10.0 meters in height above the equator; 10 cm relative station error; and 30 cm longitude error due to Earth rotation uncertainty.

## Media Calibrations

This section describes the effects of the media on the VLBI measurements, and the calibrations used to minimize the measurement error due to the media. The success of the calibrations are shown with comparisons of uncalibrated and calibrated VLBI data residuals.

Radio signal propagation is delayed by charged particles in solar plasma and in the Earth's ionosphere, and by the Earth's troposphere. Only the corruption to the VLBI downlink signal needs to be calibrated because the uplink signal, being common to each of the two recorded downlink signals, cancels out in the correlation process. The charged particle delay is proportional to the Total Electron Content (TEC) along the signal path and inversely proportional to the signal frequency squared. The TEC changes with time, inducing an error in the delay-rate measurement.

Since the charged particle delay is frequency dependent, a calibration to the delay-rate measurement can be computed with a linear combination of two delay-rates recorded at separate frequencies, S and X band. The computation for X-Band delay-rate, in Hertz, is:

$$\text{Delay-rate correction} = \frac{\dot{\phi}_x - (f_x/f_s)\dot{\phi}_s}{1 - (f_x/f_s)^2} \quad (6)$$

where  $\dot{\phi}_x$  and  $\dot{\phi}_s$  are the measured delay rates at X and S bands, and  $f_s$  and  $f_x$  are the S and X band frequencies [Wolff, 1985].

The average daytime fluctuation in the X-band zenith ionosphere delay is on the order of 0.1 mm/sec over 10 minutes [Wu, 1982]. Solar plasma induces a delay rate error on the order of 0.01 mm/sec in X-band signal phase-rate over 10 minutes,  $10^\circ$  away from the Sun [Kahn, 1988].

The S-band downlink cannot be coherently phase-tracked when the signal path is within  $5^\circ$  of the Sun due to large solar plasma induced spectral broadening and variations in the received signal phase. This will occur in the middle of Magellan's prime mission, from October 13, 1990 to November 22, 1990. To calibrate for charged particles during this period, ionospheric delay rate will be measured independently by measuring the Faraday rotation of linearly polarized VHF signals from geosynchronous satellites over the tracking stations. The TEC along the line-of-sight is deduced from these measurements, and mapped to the Magellan spacecraft or quasar line-of-sight as a function of time. [Royden, 1980].

A comparison between the dual-frequency calibrations and the Faraday rotation calibrations are shown in Figure 4. The calibrations, in Hertz, are shown for three spacecraft and three quasar scans, made up of 20 second points. These data were acquired on August 10, 1989. The Faraday calibrations agree with the mean of the dual-frequency calibrations for each 10 minute scan, but the dual-frequency method provides calibrations for charged

particle fluctuations within a 10 minute scan. The Faraday method provides calibrations for only the low-frequency variation of the ionosphere over a 10 minute scan.

The Earth's troposphere induces a radio signal delay from 2 meters at zenith, to 12 meters at 10° elevation. A seasonal model of the delays, generated from 2 years of radiosonde measurements made at the DSN tracking stations, can calibrate this delay to 6 cm in zenith, which scales to other elevation angles in proportion to the path length through the troposphere [Chao, 1971]. This model does not predict the fluctuating wet component of the troposphere well. A theoretical prediction of this error at 10° elevation is 0.07 mm/sec [Truehaft and Lanyi, 1987].

To verify the integrity of the VLBI data, the sub-second phase residuals from each station are plotted before compressing. A line is removed from these residuals, leaving only media information, so that any cycle slips can be corrected before observable generation. These plots are also useful to assess the size of media corruptions. In Figure 5, the S and X-Band phase residuals are plotted, for 3 separate 10 minute spacecraft scans, over 75 minutes on July 27, 1989. The phase received at the California station and the Madrid station are each plotted, as well as the station differenced phase. The scale is defined by the S and X wavelengths denoted on the right side of the plots. In scans 1 and 2, at both California and Spain, the same phase signatures appear, and the X-Band signature is larger than the S-Band. This is due to charged particle corruption to the uplink, which is multiplied by the spacecraft to X-Band frequency for downlink. This effect is eliminated in the station differenced phase for these scans. In scan 3, however, the phase is perturbed by the fluctuating wet troposphere, which has a larger effect at the higher X-Band frequency, and is not eliminated in the station differencing. The wet troposphere can fluctuate so fast that this effect cannot be removed by the quasar calibration, leaving this effect as the dominant VLBI error source for velocity measurements.

Figure 6 also shows phase residuals for 2 spacecraft scans, acquired over 2 hours on July 16, 1989. In both scans, the ionosphere delay over Australia is apparent because the X-Band phase signature is magnified in the S-Band phase, and remains in the station differenced phase. This effect can be completely eliminated by applying the S and X-Band dual-frequency calibration to each the spacecraft and quasar data points.

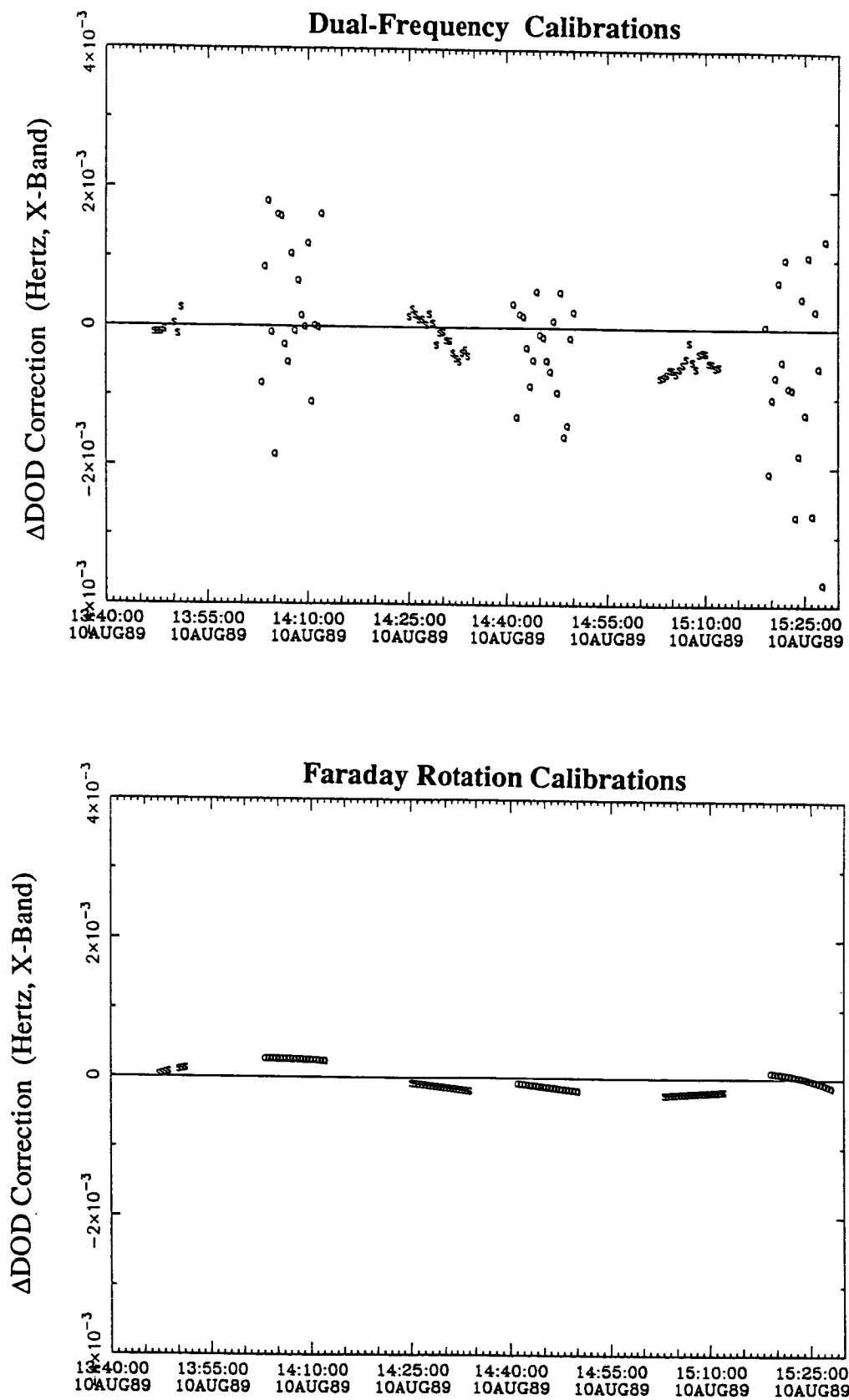
## Media Calibration Results

### DOR

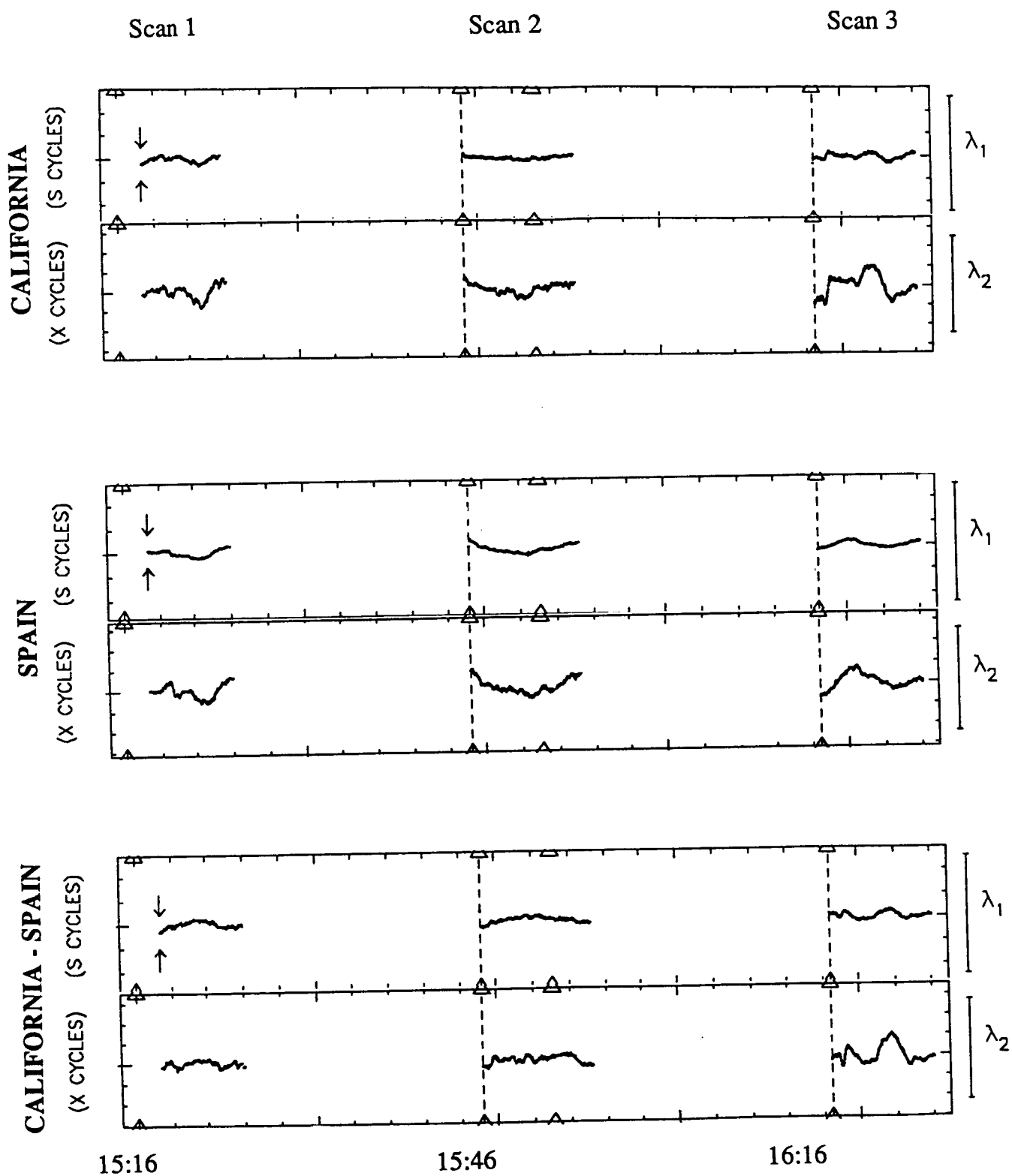
Two sets of  $\Delta$ DOR residuals, each computed with the reference trajectory described above, are shown in Figure 7. These residuals were computed with and without the seasonal troposphere calibration. The calibrated troposphere delay is about 5 meters. The post-calibration residual RMS is 0.183 meters, or 20 nanoradians in  $\theta$ , the geocentric angular position.

Figure 8 shows residuals computed with and without Faraday rotation ionosphere calibrations. This calibration improves some scans (August 6 and 8), but degrades others





**Figure 4.** Charged Particle Calibrations for August 10, 1989



**Figure 5.** Uncompressed Phase Residuals for July 27, 1989

$\lambda_1 = 131 \text{ mm}$ ,  $\lambda_2 = 36 \text{ mm}$

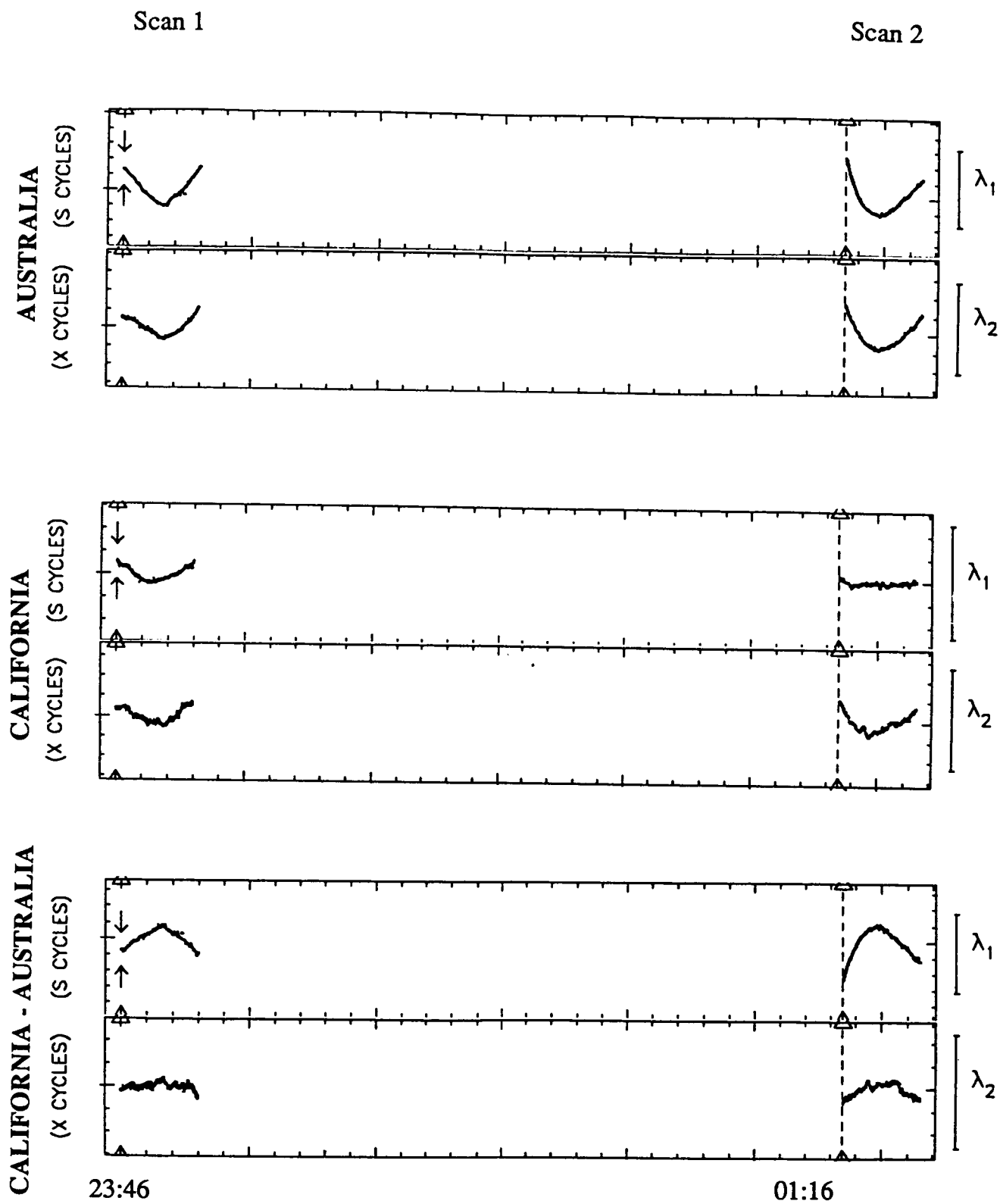


**Figure 6.** Uncompressed Phase Residuals for July 17, 1989

$$\lambda_1 = 131 \text{ mm}, \quad \lambda_2 = 36 \text{ mm}$$

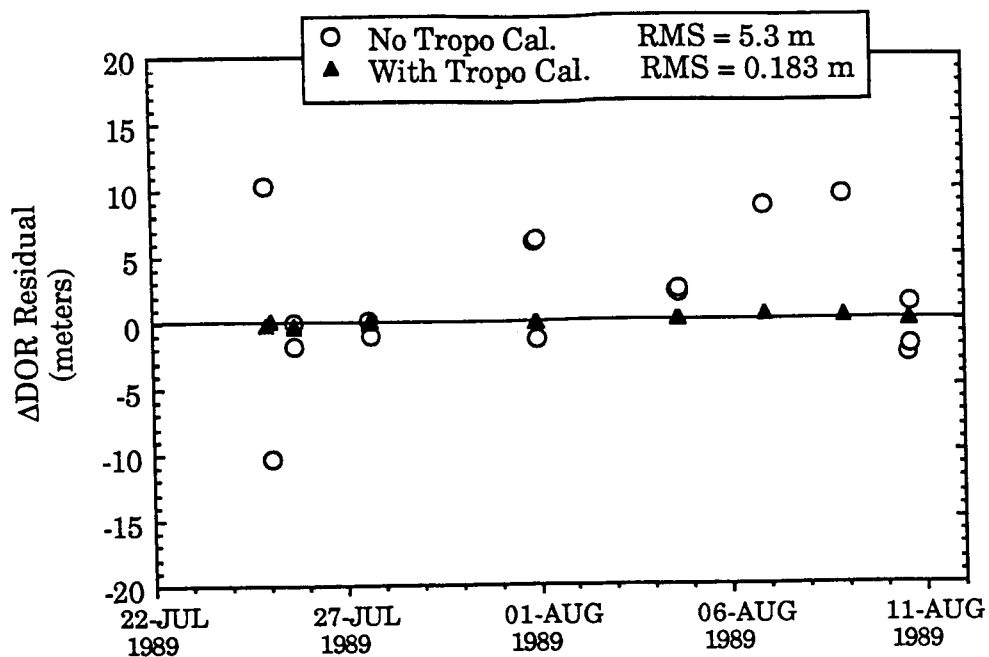


**Figure 7.** ADOR Residuals with and without Troposphere Calibration.

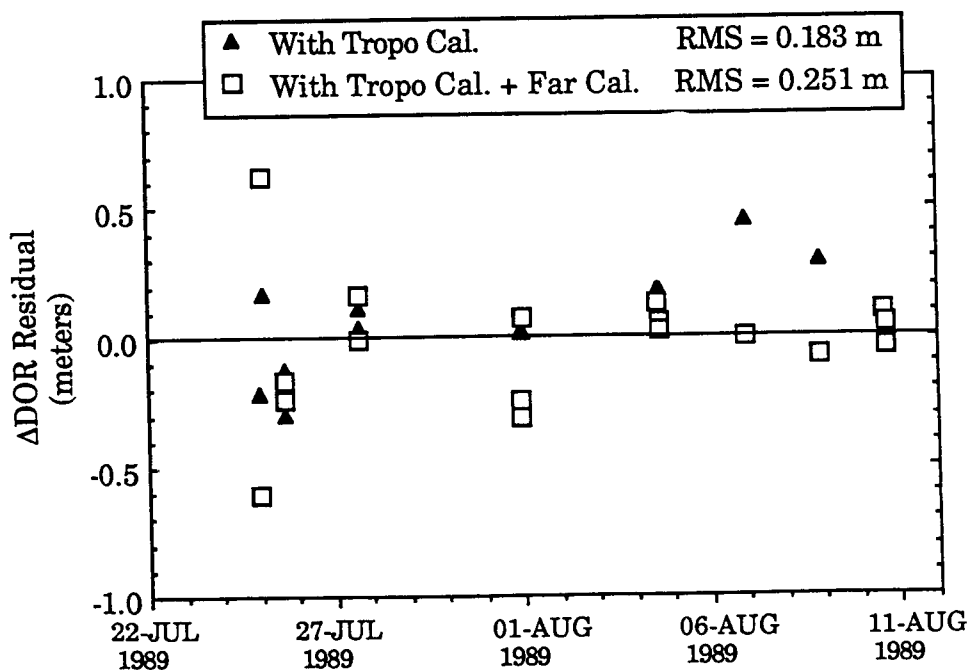


**Figure 8.** ADOR Residuals with and without Ionosphere Calibration.

(July 25), with a small net residual RMS degradation of 0.07 meters. This could be due to the error incurred when mapping the TEC from zenith to the low Magellan line-of-sight.

## DOD

Two sets of  $\Delta$ DOD residuals are shown in Figure 9. These residuals were computed with and without the seasonal troposphere calibration. The RMS troposphere delay-rate calibration is 0.66 mm/sec. The post-calibration residual RMS is 0.054 mm/sec, or 6 picoradians/sec in the geocentric angular velocity,  $\dot{\theta}$ .

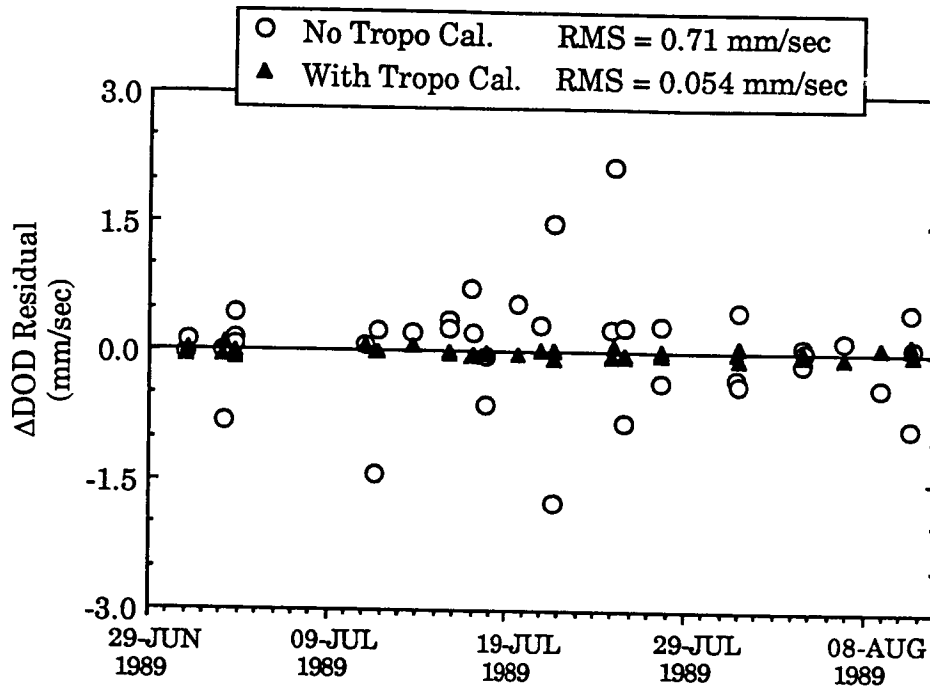


Figure 9.  $\Delta$ DOD Residuals with and without Troposphere Calibration.

The calibration improvement using the quasar DOD measurement is shown in Figure 10, which plots the DOD residuals with and without the quasar calibration. Both data sets have been calibrated with the seasonal troposphere model. The quasar calibration improves the residual RMS by 0.05 mm/sec, or about 6 picoradians/sec in  $\dot{\theta}$ , the geocentric angular velocity. The quasar calibrates the ionosphere and troposphere components common between the two scans, station location errors, and station clock drift.

Figure 11 shows two sets of  $\Delta$ DOD residuals, computed with and without charged particle calibrations. Dual-frequency (S and X-Band) calibrations were used, except for measurements where the S-Band measurement was not recorded; in these cases, the Faraday ionosphere calibration was used (20% of the data points). The charged particle calibration improves the data RMS by 0.01 mm/sec, or about 1 picoradian/sec. This is the expected delay-rate due to the solar plasma; most of the ionosphere delay-rate for this data set was calibrated with the quasar measurement. The resulting residual RMS is 0.045 mm/sec, or about 5 picoradians/sec.

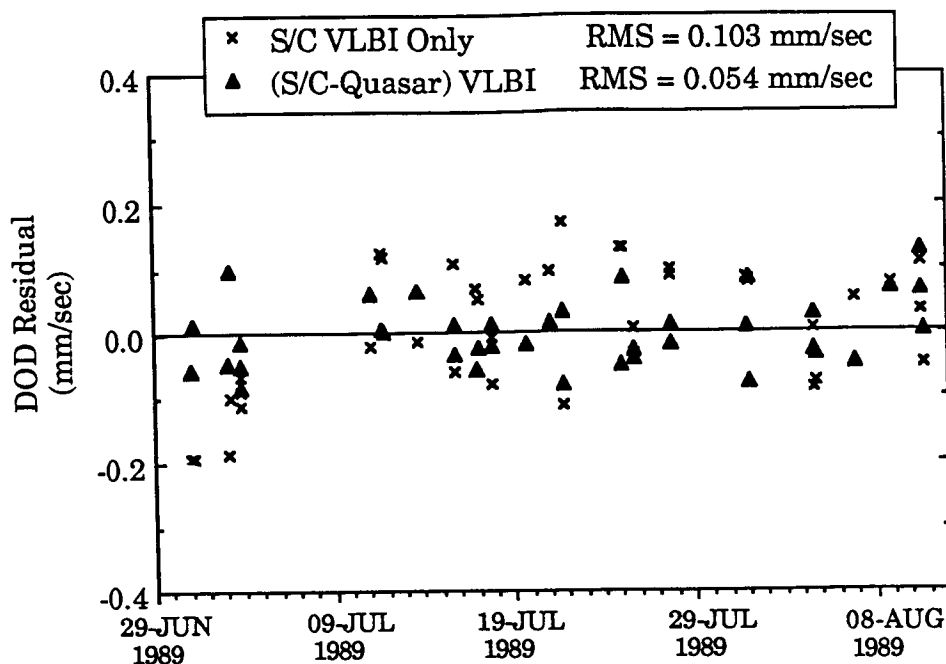
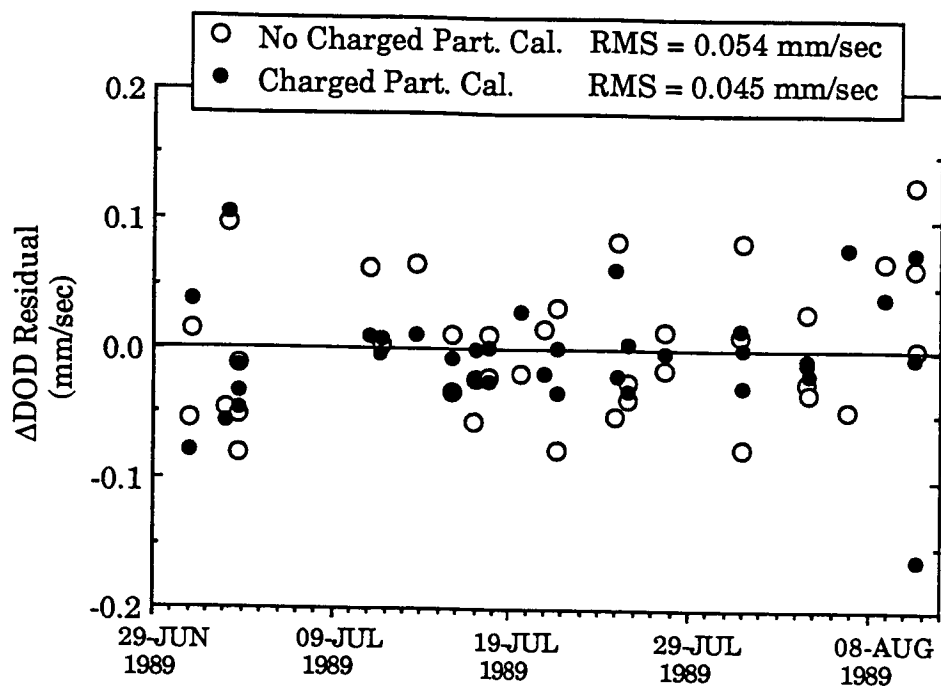


Figure 10. DOD Residuals with and without Calibration by Quasar.

#### Earth Platform Model

Errors in the tracking station location in inertial space induce errors in the computation of the  $\Delta$ VLBI signal delay and delay-rate. An error in the angular position of the quasar also contributes to the error. The tracking station locations and quasar locations used for the  $\Delta$ VLBI computations were derived from VLBI observations of quasars, and oriented to the planetary ephemeris frame. This orientation was constructed by matching the VLBI station locations to the Lunar Laser Ranging (LLR) station locations, which were used in the derivation of the planetary ephemeris reference frame [Folkner and Finger, 1989; Neill, 1984]. The uncertainty of this orientation is believed to be 20 nanoradians, though possible systematic errors are still being investigated. Figure 12 shows the  $\Delta$ DOR residuals computed with these station locations and quasar locations. The  $\Delta$ DOR residuals were also computed using tracking stations derived from planetary encounter tracking data [Moyer, 1988]. The quasar locations were oriented to this planetary frame by simply rotating the quasar right ascensions by the average offset between the longitudes of the Moyer station set and the standard VLBI station set [Ulvestad, 1989]. This average offset is 208 nanoradians. Figure 12 also shows the  $\Delta$ DOR residuals computed with these station locations and quasar locations. The  $\Delta$ DOR residual RMS was degraded by 5.4 cm, or 6 nanoradians in geocentric angular position, for this case.

The Earth's pole location and rotation rate (UT1) fluctuate due to deformations of the



**Figure 11.** ΔDOD Residuals with and without Charged Particle Calibration.

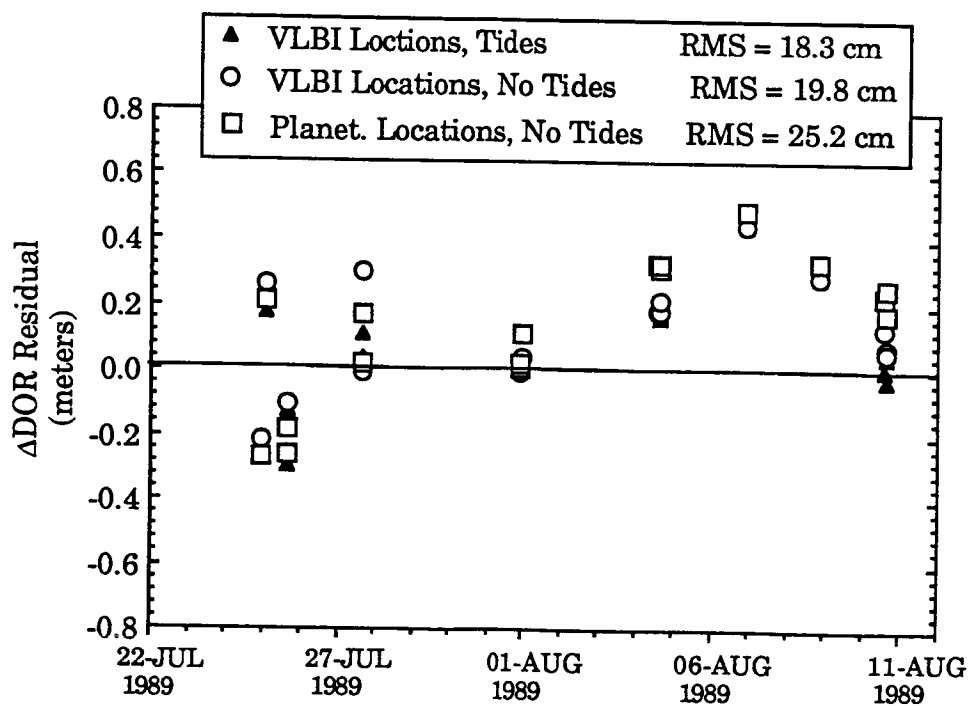


**Figure 12.** ΔDOR Residuals with alternate Earth Platform Models.

solid Earth and by exchanges of angular momentum between the solid and fluid parts of the Earth, as well as by exchanges of angular momentum with extraterrestrial objects. This motion is estimated using several sources of geodetic measurements. A Kalman filtering solution produces a smoothed time series with interpolation points spaced every 2 weeks. Tidal deformation of the Earth by the sun and moon produce periodic variations in the Earth's moment of inertia, and therefore in the Earth's rotation rate. These short-term tidal effects can be calculated from a theoretical model [Yoder et al., 1981], and included in this time series, with interpolation points every 2 days. Figure 12 shows  $\Delta$ DOR residuals computed with and without these tidal effects. Inclusion of these tidal terms improved the residual RMS by 1.5 cm, or 1.7 nanoradians.

These improved levels of Earth platform modelling did not improve the  $\Delta$ DOD measurement accuracy. As shown in Figure 12, these model improvements only provided slight improvement to the  $\Delta$ DOR measurement accuracy.

### Conclusions

Measurements of the Magellan spacecraft angular position and velocity are were made with  $\Delta$ VLBI during the the spacecraft's heliocentric cruise from Earth to Venus. The angular measurement accuracy was 20 nanoradians in position and 5 picoradians/sec in velocity. The largest error contribution for velocity comes from the fluctuating wet troposphere; this media effect fluctuates too quickly to be calibrated with the quasar measurement. Charged particle effects are eliminated by dual-frequency calibrations. Faraday rotation measurements provide effective ionosphere calibrations when dual-frequency measurements are not available. Small improvements in the  $\Delta$ DOR measurement accuracy, on the order of a few nanoradians, were obtained with an Earth platform model containing tracking station locations derived from quasar VLBI observations versus stations locations derived from planetary encounter tracking data. Modelling the high frequency effects in the Earth rotation model due to the solid Earth tides also improves the  $\Delta$ DOR measurement accuracy by a few nanoradians. Each of these Earth platform models did not improve the  $\Delta$ DOD measurement accuracy for this data set.

### Acknowledgement

The work described in this paper was carried out at the Jet Propulsion Laboratory, California Institute of Technology, under contract with the National Aeronautics and Astronautics Administration.

### References

Border, J.S., F.F. Dovivan, S.G. Finley, C.E. Hildebrand, B. Moultrie, and L.J. Skjerve, "Determining Spacecraft Angular Position with Delta VLBI: The Voyager Demonstration", paper AIAA-82-1471, AIAA/AAS Astrodynamics Conference, San Diego, California, August, 1982.



- Chao, C.C., "New Troposphere Range Corrections with Seasonal Adjustment", JPL Technical Report 32-1526, V. 6, pp.67-82, Jet Propulsion Laboratory, September/October 1971.
- Esposito, P.B., F.F. Donovan, S.G. Finley, X.X. Newhall, C.B. Smith, S.C. Wu, "Narrow-band Differential Interferometry Applied to Pioneer Venus Orbiter", AAS paper 83-310, AAS/AIAA Astrodynamics Specialist Conference, Lake Placid, New York, August, 1983.
- Folkner, W.M., and M.H. Finger, "Station Location set and quasar catalog for use with ephemeris DE200", JPL internal document, September, 1989.
- Kahn, R.D., and J.S. Border, "Precise Interferometric Tracking of Spacecraft at Low Sun-Earth-Probe Angles", paper AIAA-88-0572, AIAA 26th Aerospace Sciences Meeting, Reno, Nevada, January, 1988.
- Melbourne, W.G., and D.W. Curkendall, "Radiometric Direction Finding: A New Approach to Deep Space Navigation", paper A78-31889, AAS/AIAA Astrodynamics Specialist Conference, Jackson Hole, Wyoming, September, 1977.
- Moyer, T.D., "J2000 Station Location Sets for Planetary Ephemerides DE200 and DE202 and 1950 Station Coordinates for DE130", JPL internal document, August, 1988.
- Mohan, S.N., "Challenges In Navigation of the Venus Radar Mapper (VRM) Spacecraft", paper IAF-85-259, IAF '85, Stockholm, Sweden, October, 1985.
- Neill, A.E., "Absolute Geocentric DSN Station Locations and Radio-Planetary Frame Tie", JPL internal document, March, 1984.
- Royden, H.N., D.W. Green, G.R. Walson, "Use of Faraday-Rotation Data from Beacon Satellites to Determine Ionospheric Corrections for Interplanetary Spacecraft Navigation", Proc. Satellite Beacon Symposium, Warszawa, Poland, May, 1980.
- Thomas, J.B., "An Analysis of Long Baseline Radio Interferometry", JPL Technical Report 32-1526, Vol. VII, pp. 37-50, 1972.
- Treuhaft, R.N. and G.E. Lanyi, "The effect of the dynamic wet troposphere on radio interferometric measurements", *Radio Science*, Volume 22, Number 2, pp. 251-265, March-April 1987.
- Ulvestad, J.S. and O.J. Sovers, "Preliminary VLBI catalog for Magellan", JPL internal document, January, 1989.
- Wood, L.J., "Orbit Determination Singularities in the Doppler Tracking of a Planetary Orbiter", *Journal of Guidance, Control, and Dynamics*, Volume 9, Number 4, page 485, July-August 1986.

Wolff, P.J., "Documentation of the equations in the CALGEN Program", JPL internal document, September, 1985.

Wu, S.C., "Error Estimation for  $\Delta$ VLBI Angle and Angle Rate Measurements Over Baselines Between a Ground Station and a Geosynchronous Orbiter", TDA Progress Report 42-71, pp. 8-19, July-September 1982.

Yoder, C.F., J.G. Williams, M.E. Parke, "Tidal Variations of Earth Rotation", *Journal of Geophysical Research*, pp. 881-891, 1981.